

Automatic Reconstruction of As-built BIM from Laser Scanned Data of Precast Concrete Elements for Dimensional Quality Assessment

Q. Wang^{a,b}, J. C. P. Cheng^a and H. Sohn^b

^aDepartment of Civil and Environmental Engineering,
The Hong Kong University of Science and Technology, Hong Kong

^bDepartment of Civil and Environmental Engineering,
Korea Advanced Institute of Science and Technology, South Korea
E-mail: qwangau@ust.hk, cejcheng@ust.hk, hoonsohn@kaist.ac.kr

Abstract –

Precast concrete elements are popularly used in the construction of buildings and infrastructures because they enable higher construction quality, less construction time, and less environmental impact. To ensure the performance of complete precast concrete systems, dimensional quality of individual precast concrete elements must be assessed before they are transported to the construction sites. However, the current quality assessment methods mainly rely on manual inspection with traditional measurement devices, which are inefficient and inaccurate. Besides, the quality assessment results are not well managed. To realize efficient and accurate quality assessment of precast concrete elements and to facilitate the management of quality assessment results, this study proposes a technique which can automatically reconstruct the as-built Building Information Models (BIM) from laser scan data of precast concrete elements for dimensional quality assessment. The proposed technique firstly performs a scan planning to determine the number of scans and the locations of scanners. Then, the pre-processing of scan data removes noisy data and registers multiple scans in a global coordinate system. Afterwards, the as-built geometries of the element are extracted from the registered scan data, and finally the as-built BIM is reconstructed. To validate the proposed technique, a scanning experiment was conducted on a small-scale test specimen. The experimental results demonstrate that the proposed technique can accurately and efficiently create as-built BIM of precast concrete elements.

Keywords –

Building Information Models; Laser scanning; As-built BIM reconstruction; Precast concrete elements; Quality assessment

1 Introduction

Precast concrete elements are popularly used in the construction of buildings and infrastructures because they enable higher construction quality, less construction time, and less environmental impact, compared to cast-in-place concrete [1, 2]. To ensure the performance of complete precast concrete systems, the dimensions of individual precast concrete elements must be assessed before they are transported to the construction sites. However, the current quality assessment of precast concrete elements is mainly performed manually using traditional devices such as measuring tapes. Such traditional quality assessment methods are proven to be time-consuming and error-prone [3]. Besides, as the quality assessment results are traditionally recorded in paper sheets or electronic spreadsheets, the as-built conditions of the elements are not well managed in a long term.

These days, 3D laser scanners have become popular in civil engineering because they can acquire 3D range measurement data, known as point cloud data, at a high speed of million scan points per second and with a high accuracy up to a few millimeters. Utilizing laser scan data, a variety of applications have been reported, including 3D model reconstruction [4, 5], construction progress monitoring [6, 7], structural quality assessment [8, 9], etc. On the other hand, Building Information Models (BIM) have become a trend in the Architecture, Engineering, and Construction/Facility Management (AEC/FM) industry because BIM facilitates the storage, visualization, and management of building information

throughout the whole lifecycle of a facility.

To achieve efficient and accurate quality assessment of precast concrete elements and to facilitate the management of quality assessment results, this study proposes a technique that can automatically reconstruct the as-built BIM of precast concrete elements, particularly focused on precast concrete bridge deck panels. The as-built BIM representing the as-built conditions of an element can be compared to the corresponding as-design blueprints or models for dimensional quality assessment. Furthermore, the as-built BIM can facilitate the assemblage, maintenance, and replacement of the precast concrete element. This paper is organized as follows. Section 2 provides background information on (1) the existing research on BIM reconstruction from laser scan data, and (2) the precast concrete bridge deck panels. Then, the proposed technique for automatic as-built BIM reconstruction is presented in Section 3, and an experimental validation of the proposed technique is described in Section 4. Finally, Section 5 concludes this study and suggests future work.

2 Background

2.1 BIM reconstruction from laser scan data

While manual BIM reconstruction from laser scan data is time-consuming and labor-intensive, a few studies have developed algorithms for automatic BIM reconstruction. The main challenges and research topics for automatic BIM reconstruction include (1) the registration of multiple scans, (2) geometric modeling, and (3) object recognition.

To generate a complete point cloud covering all the surfaces of a target, multiple scans must be conducted at different locations. Then, the scan data obtained from different scans are aligned in a global coordinate system during the registration process of multiple scans. Although automatic registration methods have been developed in computer vision area, they are not applicable to the AEC/FM industry [10]. Instead, considering that most surfaces are planar in the AEC/FM context, some studies have developed automatic or semi-automatic plane-based registration methods, which register two scans by matching their common plane [11, 12].

Geometric modeling refers to the process of detecting and modeling certain geometry shapes from the scan data. The most common shape in the AEC/FM context is plane. A number of algorithms have been adopted to detect planes, including the RANSAC algorithm [11], the Hough transform [13], and the region-growing algorithm [5]. Besides planar surfaces,

cylindrical shapes, which can represent pipes and some conduits, have also been studied [14].

Object recognition aims to recognize specific construction components, e.g., wall, roof, column, etc., from the detected geometry shapes. Several approaches for automatic object recognition have been investigated, including machine learning algorithms [5], context-based recognition [15], and the use of prior knowledge [16].

2.2 Precast concrete bridge deck panels

Precast concrete bridge decks have been used successfully for several decades. Along with the reduction of construction time, the quick replacement of precast concrete bridge decks also reduces the impact on traffic flow significantly, which is essential in urban areas. A precast concrete bridge deck consists of a series of bridge deck panels, which are connected one by one. To connect panels with the girders and to connect adjacent panels, three structural features, namely shear pockets, shear keys and flat ducts, are usually provided on the bridge deck panels, as shown in Figures 1(a)-(b).

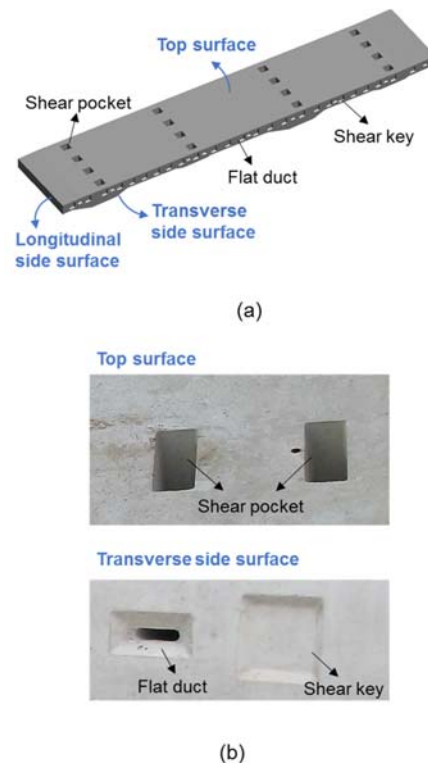


Figure 1. Precast concrete bridge deck panels. (a) A 3D model of a bridge deck panel. (b) Examples of shear pocket, flat duct, and shear key on an actual bridge deck panel.

Shear pockets are provided on the top surface of a panel and they usually have rectangular shapes. They serve as panel-to-girder joints after grout is filled inside. Shear keys are distributed along the transverse side surfaces of panels and serve as transverse panel-to-panel joints. They are designed to eliminate relative vertical movement between adjacent panels. Shear keys are mainly in two categories, non-grouted match-case shear keys using epoxy adhesive and grouted female-to-female shear keys, and the one shown in Fig. 1(b) is the latter. Female-to-female shear keys use grout to fill the joints between adjacent panels to achieve the required strength. Last, ducts are also distributed along the transverse side surfaces of panels. They are used to place post-tensioned longitudinal reinforcements, which put the transverse panel-to-panel joints under compression and eliminate the tensile stress resulting from the live load. Ducts are usually rounded or flat in shape, and the one shown in Fig. 1(b) is a flat duct.

3 Proposed technique for automatic reconstruction of as-built BIM

Figure 2 illustrates the procedures of the proposed technique based on laser scanning for automatic as-built BIM reconstruction. The proposed technique includes four steps: (1) scan planning, (2) scan data pre-processing, (3) extraction of geometry, and (4) reconstruction of as-built BIM. The details of the four steps are illustrated in Sections 3.1-3.4, respectively.

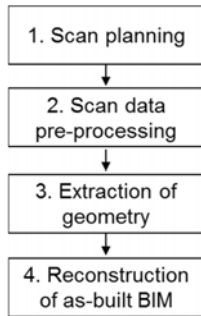


Figure 2. Procedures of the proposed technique based on laser scanning for automatic as-built BIM reconstruction

3.1 Scan planning

To acquire scan data covering all the surfaces of an element, multiple scans must be conducted at different locations. To obtain high resolution scan data and to save scanning time, scan planning is performed to minimize the number of scans and to optimize the

locations of the scanner. The set of scans, namely scan set, must meet the following two requirements.

(1) For any arbitrary point on the target, there should exist at least one scan that provides high resolution scan data surrounding this point. Here, high resolution scan data require that the spacing s between two adjacent scan points is less than a threshold value S_T .

(2) Scan data from all the scans should be able to be registered based on common planes. This is motivated by that a plane-based registration will be adopted in the proposed technique to register multiple scans. Assuming that a total of four planes, P1, P2, P3, and P4, need to be scanned, and a total of three scans, S1, S2, and S3, are conducted, two different cases are illustrated in Figure 3. In case 1, S1 covers P1 and P2, S2 covers P2 and P4, and S3 covers P3 and P4. Therefore, firstly S1 and S2 can be registered based on their common plane P2; and then the registered scan data can be further registered with S3 based on their common plane P4. However, in case 2, although S1 and S2 can be registered, S3 cannot be registered with any other scan. Therefore, the scan set in case 2 does not meet requirement (2).

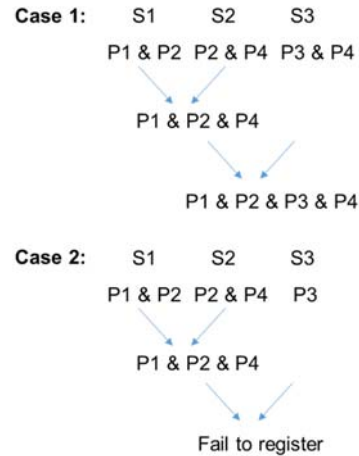


Figure 3. All the scans should be able to be registered by common planes: case 1 is a success case and case 2 is a failure case

Among all the scan sets that fulfill the above requirements, the ones that contain the minimum number of scans are firstly found. Here, the minimum number of scans is denoted as N_{min} . Then, among all the scan sets with N_{min} scans, the one that brings the smallest averaged s value is selected.

3.2 Scan data pre-processing

After the scan data are acquired at the planned

scanning locations, the scan data pre-processing is performed, which consists of filtering of noisy data and registration of scans, as illustrated in Sections 3.2.1 and 3.2.2, respectively.

3.2.1 Filtering of noisy data

Raw scan data contain three types of scan points – (1) valid points belonging to the target object, (2) background points belonging to the background objects, and (3) erroneous data points called mixed pixels. A mixed pixel occurs when a laser beam emitted at the edge of an object is split into two parts and falls on two different surfaces. The two reflected signals are both received by the scanner and the resulting scan point becomes a mixed pixel. Hence, the filtering of noisy data aims to remove both mixed pixels and background points, while retaining valid points only.

Although mixed pixels can be anywhere along the direction of the laser beam, they usually have a lower spatial density compared to valid points or background points [17]. Therefore, a density-based clustering algorithm, namely the density-based spatial clustering of applications with noise (DBSCAN) [18], is adopted to filter out mixed pixels and background points, which is proven to be effective in [19]. After applying the DBSCAN algorithm, mixed pixels are classified as noise due to the low density, valid points become one cluster due to the high density, and background points become one or multiple clusters, depending on the specific background objects. Finally, among all the clusters of points, the one that has the least average distance to the scanner is identified as valid points.

3.2.2 Registration of scans

The registration of scans includes two steps – (1) a coarse registration which provides a rough alignment of scans, and (2) a fine registration which further improves the initial solution.

The coarse registration aligns two scans based on their common plane. For a typical bridge deck panel, five planes (the top surface, two transverse side surfaces, and two longitudinal side surfaces, as shown in Figure 1(a)) are used for coarse registration. Firstly, for each scan, all the planes are detected from the scan data using the RANSAC [20] algorithm. Then, the common plane of the two scans is identified. If two scans have more than one common plane, the one with the largest size is used for registration. In case that one scan covers two or three planes, the correct common plane is identified based on the sizes of planes, because the top, the transverse side, and the longitudinal side surfaces of a panel have substantially different sizes. Thirdly, for the common plane, its mass center (O) and three

eigenvectors (e_1 , e_2 and e_3) are obtained from both scans, as shown in Figure 4. Lastly, the two scans are aligned by making the mass center and eigenvectors of their common plane coincident.

After coarse registration, the point-to-plane Iterative Closet Point (ICP) [21] algorithm is used for fine registration, which optimizes the registration results by minimizing the point-to-plane distances between the two scans.

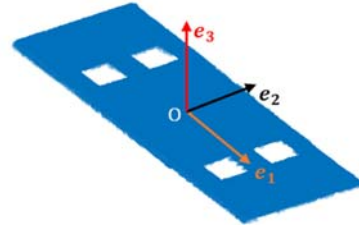


Figure 4. The mass center (O) and the eigenvectors (e_1 , e_2 and e_3) of a plane

3.3 Extraction of geometry

To create the as-built BIM, the necessary geometric information of the element needs to be extracted from the registered scan data, including the dimensions and locations of shear pockets, flat ducts, and shear keys, and the dimensions of the outer boundaries of the element.

3.3.1 Extraction of shear pockets and flat ducts

Shear pockets and flat ducts are basically holes that go through the element. Hence, in the scan data, they are characterized by areas without any scan point. In the following explanations, the shear pockets on the top surface are taken as the example, and the flat ducts can be extracted in a similar way.

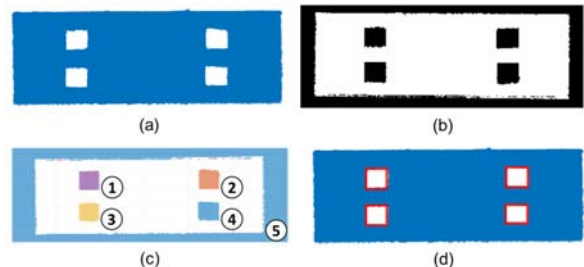


Figure 5. Extraction of shear pockets from scan data. (a) The scan data of the top surface. (b) Binary image of the top surface. (c) Detection of shear pockets. (d) Extraction of the edges of the

shear pockets.

First, the scan data of the top surface (Figure 5(a)) are transformed into a binary image (Figure 5(b)), where white pixels represent areas with scan points and black pixels represent areas without any scan point. Then, the black areas are clustered by the DBSCAN algorithm and the areas are classified into five clusters, which are denoted as clusters 1-5 and shown in different colors in Figure 5(c). Among all the five clusters, only the ones with proper sizes are identified as shear pockets. Such proper sizes are determined based on an estimation of the actual sizes of the shear pockets. Therefore, clusters 1-4 are identified as shear pockets, whereas cluster 5 is ignored due to its too large size. Last, based on the locations of the shear pockets, the four edges of each shear pocket are estimated using the edge line estimation algorithm proposed in [19], as shown in red lines in Figure 5(d).

3.3.2 Extraction of shear keys

A typical shear key has six surface in its local area, as shown in Figure 6(a). Among them, surfaces 5 and 6 have the same normal vector \vec{n} , whereas surfaces 1-4 have normal vectors which have 45° difference from \vec{n} . Based on this observation, shear keys on the transverse side surface are extracted as follows.

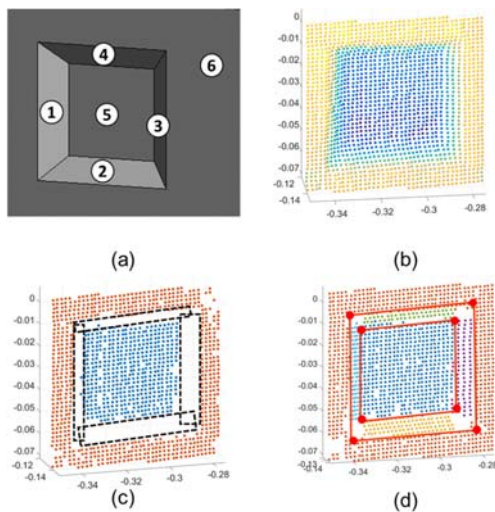


Figure 6. Extraction of shear keys from scan data. (a) The 6 surfaces in the local area of a shear key. (b) The scan data surrounding a shear key. (c) The scan points for surfaces 5 (blue dots) and 6 (orange dots), and the estimated areas of surfaces 1-4 (dashed boxes). (d) The scan points for all six surfaces (in different colors) and the

extracted corner points (red dots) of the shear key.

First, the normal vector \vec{n} of surface 6 is estimated as the normal of the least-squares fitting plane of all the scan points (Figure 6(b)) on the transverse side surface. Then, the scan points, the local normal vectors of which have large differences from \vec{n} , are filtered out. Here, scan points representing surfaces 1-4 are expected to be removed. The remaining scan points are further classified by the DBSCAN algorithm into two clusters, which represent surfaces 5 and 6, respectively, as shown in Figure 6(c). Once the scan points for surfaces 5 and 6 are obtained, the areas of surfaces 1-4 can be estimated between them, as shown in dashed boxes in Figure 6(c). Last, for each surface among surfaces 1-4, a plane is detected by the RANSAC algorithm using scan points within its estimated area. As shown in Figure 6(d), the scan points representing all the 6 surfaces are shown in different colors and each corner point (shown in red dots in Figure 6(d)) of the shear key is obtained by intersecting three surfaces surrounding this corner point.

3.3.3 Extraction of outer boundaries

Although the outer boundaries are designed to be straight lines, the as-built conditions can be different. To reflect the actual conditions, a set of points are extracted along each boundary to represent it. As shown in Figure 7, surfaces SF1 and SF2 intersect at the boundary B1. With an interval of q , a set of boundary points are obtained to represent B1, as shown in red dots. Each boundary point is obtained as the intersection point of 3 planes, i.e., the local fitting plane of scan points on SF1 (shown in green), the local fitting plane of scan points on SF2 (shown in blue), and the cross section plane perpendicular to both SF1 and SF2.

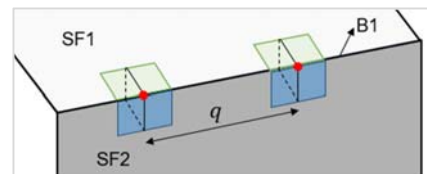


Figure 7. Extraction of a set of boundary points (shown as red dots) representing the actual conditions of boundary B1

3.4 Reconstruction of as-built BIM

To facilitate data exchange among different stakeholders throughout the lifecycle, a neutral BIM data model, namely Industry Foundation Classes (IFC),

is adopted to create the as-built BIM. Because the geometry of bridge deck panels is complex, the panel is divided into several units and modelled separately. Each shear pocket, flat duct, or shear key becomes one unit, and the panel itself excluding all the above-mentioned structural features becomes another unit. First, for each single unit, its geometry is triangulated and represented by an instance of *IfcFacetedBrep*, which represents a geometry by a set of connected surfaces. Then, an instance of *IfcBooleanResult* is created, which can represent the difference (or other Boolean operators) of two *IfcFacetedBrep* instances. For example, Figure 8(a) shows two *IfcFacetedBrep* instances and Figure 8(b) shows their difference using an *IfcBooleanResult* instance. Therefore, when one instance is set as the unit of the panel itself and the other is set as the units of all structural features, the panel with all structural features can be represented by the *IfcBooleanResult* instance.

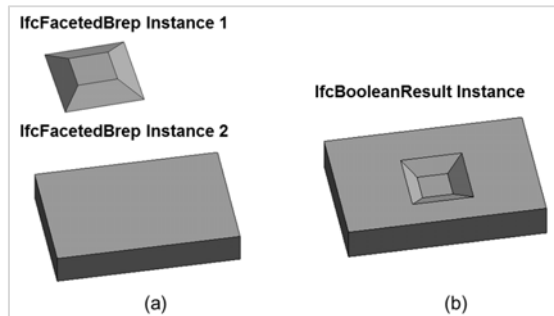


Figure 8. Geometry representation using IFC format. (a) Two *IfcFacetedBrep* instances. (b) An *IfcBooleanResult* instance representing the difference of the two *IfcFacetedBrep* instances.

4 Experimental validation

4.1 Test specimen

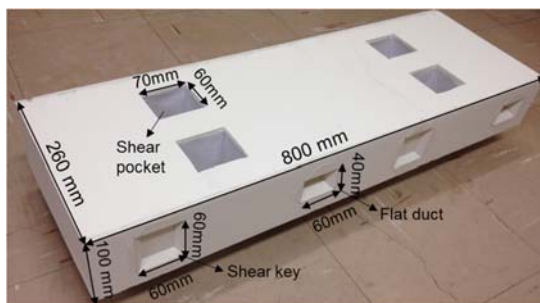


Figure 9. Dimensions of the test specimen

To validate the proposed technique of automatic as-built BIM reconstruction, a small-scale test specimen was manufactured in the laboratory using Styrofoam materials. As shown in Figure 9, the test specimen had dimensions of 800 mm (length) \times 260 mm (width) \times 100 mm (height). On the top surface, there were a total of 4 shear pockets, with identical dimensions of 70 mm \times 60 mm. On each transverse side surface, there were a total of 2 flat ducts and 2 shear keys, with identical outer dimensions of 60 mm \times 60 mm and 60 mm \times 40 mm, respectively.

4.2 Applying the proposed technique

The proposed technique was applied to reconstruct the as-built BIM of the test specimen. In this experiment, all the surfaces, except the bottom surface, of the specimen need to be scanned.

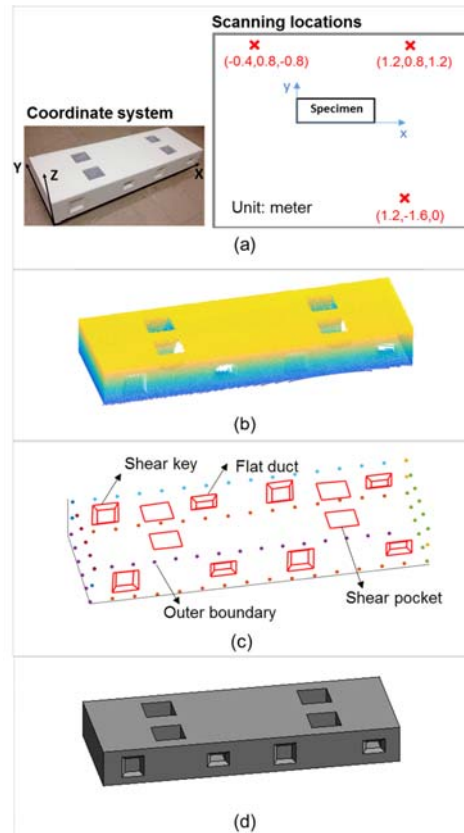


Figure 10. Applying the proposed technique on the test specimen. (a) The XYZ coordinates of the optimal set of scanning locations. (b) The scan data after data pre-processing. (c) The extracted geometries. (d) The reconstructed as-built BIM of the test specimen.

First, in the scan planning, the angular resolution was set as 0.036° and the spacing threshold S_T was set as 2 mm. Then the minimum number of scans was solved as 3 and the XYZ coordinates (unit: meter) of the optimized set of scanning locations are (-0.4, 0.8, -0.8), (1.2, 0.8, 1.2), and (1.2, -1.6, 0), as shown in Figure 10(a). Since the scanning locations are solved from an exhaustive search among a set of possible scanning locations, the solution is approximately optimized. In this study, a FARO Focus 3D terrestrial laser scanner was used to acquire the scan data. Then, by data pre-processing, the scan data from all the three scans were filtered and registered, and the obtained scan data are shown in Figure 10(b). Afterwards, the geometries of the test specimen, including shear pockets, flat ducts, shear keys, and the outer boundaries, were extracted from the registered scan data, as shown in Figure 10(c). Lastly, based on the extracted geometries, the as-built BIM of the specimen was created with the IFC data model, as shown in Figure 10(d).

4.3 Accuracy of the as-built BIM

To examine the accuracy of the created as-built BIM, the dimensions of the specimen in the as-built BIM were compared to the actual dimensions, which were measured using a measuring tape with the smallest division of 1 mm. The dimensions selected for comparison include (1) the dimensions of the structural features, i.e., shear pockets, flat ducts, and shear keys, (2) the dimensions of the outer boundaries of the specimen, and (3) the locations of the structural features, e.g., the location of a shear pocket is measured as the distance from the center of the shear pocket to the outer boundaries of the top surface. The comparison results show that, for the above-mentioned three categories of dimensions, the average discrepancies between the as-built BIM and the actual dimensions are 0.8 mm, 1.6 mm, and 1.3 mm, respectively. Considering that the tolerance values for constructions are usually more than 5 mm, the as-built BIM can provide accurate as-built dimensions for dimensional quality assessment.

5 Conclusions

To conduct quality assessment of precast concrete elements in an efficient and accurate manner and to facilitate the management of the quality assessment results, this study develops a technique for automatic reconstruction of the as-built BIM of precast concrete elements from laser scan data. Particularly, this study focuses on the precast concrete bridge deck panels, which have structural features with complex geometries, including shear pockets, shear keys, and flat ducts. The

proposed technique first determines the minimum number of scans and the optimal locations of scanners. Then, data pre-processing removes noisy data and registers scan data using a plane-based approach. Third, the geometric information of the element is extracted from the scan data. Finally, the as-built BIM is created based on the extracted geometric information using the IFC data model. A small-scale test specimen was manufactured and the proposed technique was applied to the specimen to validate the proposed technique. After the as-built BIM of the specimen was reconstructed, the dimensions of the specimen stored in the as-built BIM were compared to the actual dimensions, showing an average discrepancy of around 1 mm. Therefore, it is demonstrated that the proposed technique can create the as-built BIM of precast concrete elements efficiently and accurately.

However, this study still has the following limitations. (1) Though the proposed technique is validated through small-scale specimen, its applicability needs to be further examined on real precast concrete elements. (2) This study currently focuses on a particular type of precast concrete elements, i.e., precast concrete bridge deck panels, thereby future research is needed to extend the proposed technique to other types of elements.

Acknowledgement

This research was supported by a grant (13SCIPA01) from Smart Civil Infrastructure Research Program funded by Ministry of Land, Infrastructure and Transport (MOLIT) of Korea government and Korea Agency for Infrastructure Technology Advancement (KAIA).

References

1. Glass, J., B.P.C. Federation, and B.C. Association, *The future for precast concrete in low-rise housing*. 2000: British Precast Concrete Federation Leicester.
2. Tadros, M.K. and M.C. Baishya, *Rapid replacement of bridge decks*. Vol. 407. 1998: Transportation Research Board.
3. Phares, B. M., Washer, G. A., Rolander, D. D., Graybeal, B. A., & Moore, M. (2004). Routine highway bridge inspection condition documentation accuracy and reliability. *Journal of Bridge Engineering*, 9(4), 403-413.
4. Tang, P., Huber, D., Akinci, B., Lipman, R., & Lytle, A. (2010). Automatic reconstruction of as-built building information models from

- laser-scanned point clouds: A review of related techniques. *Automation in construction*, 19(7), 829-843.
5. Xiong, X., Adan, A., Akinci, B., & Huber, D. (2013). Automatic creation of semantically rich 3D building models from laser scanner data. *Automation in Construction*, 31, 325-337.
 6. El-Omari, S., & Moselhi, O. (2008). Integrating 3D laser scanning and photogrammetry for progress measurement of construction work. *Automation in construction*, 18(1), 1-9.
 7. Turkan, Y., Bosche, F., Haas, C. T., & Haas, R. (2012). Automated progress tracking using 4D schedule and 3D sensing technologies. *Automation in Construction*, 22, 414-421.
 8. Kim, M. K., Sohn, H., & Chang, C. C. (2014). Automated dimensional quality assessment of precast concrete panels using terrestrial laser scanning. *Automation in Construction*, 45, 163-177.
 9. Bosché, F. (2010). Automated recognition of 3D CAD model objects in laser scans and calculation of as-built dimensions for dimensional compliance control in construction. *Advanced engineering informatics*, 24(1), 107-118.
 10. Makadia, A., Patterson, A., & Daniilidis, K. (2006, June). Fully automatic registration of 3D point clouds. In *Computer Vision and Pattern Recognition, 2006 IEEE Computer Society Conference on* (Vol. 1, pp. 1297-1304). IEEE.
 11. Bosché, F. (2012). Plane-based registration of construction laser scans with 3D/4D building models. *Advanced Engineering Informatics*, 26(1), 90-102.
 12. Dold, C., & Brenner, C. (2006). Registration of terrestrial laser scanning data using planar patches and image data. *International Archives of Photogrammetry, Remote Sensing and Spatial Information Sciences*, 36(5), 78-83.
 13. Tarsha-Kurdi, F., Landes, T., & Grussenmeyer, P. (2007, September). Hough-transform and extended ransac algorithms for automatic detection of 3d building roof planes from lidar data. In *Proceedings of the ISPRS Workshop on Laser Scanning* (Vol. 36, pp. 407-412).
 14. Bosché, F., Ahmed, M., Turkan, Y., Haas, C. T., & Haas, R. (2015). The value of integrating Scan-to-BIM and Scan-vs-BIM techniques for construction monitoring using laser scanning and BIM: The case of cylindrical MEP components. *Automation in Construction*, 49, 201-213.
 15. Pu, S., & Vosselman, G. (2009). Knowledge based reconstruction of building models from terrestrial laser scanning data. *ISPRS Journal of Photogrammetry and Remote Sensing*, 64(6), 575-584.
 16. Vosselman, G., & Dijkman, S. (2001). 3D building model reconstruction from point clouds and ground plans. *International archives of photogrammetry remote sensing and spatial information sciences*, 34(3/W4), 37-44.
 17. Hebert, M., & Krotkov, E. (1992). 3D measurements from imaging laser radars: how good are they?. *Image and Vision Computing*, 10(3), 170-178.
 18. Ester, M., Kriegel, H. P., Sander, J., & Xu, X. (1996, August). A density-based algorithm for discovering clusters in large spatial databases with noise. In *Kdd* (Vol. 96, No. 34, pp. 226-231).
 19. Wang, Q., Kim, M. K., Cheng, J. C., & Sohn, H. (2016). Automated quality assessment of precast concrete elements with geometry irregularities using terrestrial laser scanning. *Automation in Construction*.
 20. Fischler, M. A., & Bolles, R. C. (1981). Random sample consensus: a paradigm for model fitting with applications to image analysis and automated cartography. *Communications of the ACM*, 24(6), 381-395.
 21. Chen, Y., & Medioni, G. (1992). Object modelling by registration of multiple range images. *Image and vision computing*, 10(3), 145-155.